

# MICROSTRUCTURAL EVOLUTION OF AA7050 AL ALLOY PROCESSED BY ECAP<sup>1</sup>

Kátia Regina Cardoso<sup>2</sup>  
Vanessa Guido<sup>3</sup>  
Gilbert Silva<sup>4</sup>  
Walter José Botta Filho<sup>5</sup>  
Alberto Moreira Jorge Junior<sup>6</sup>

## Abstract

This work aimed to study the microstructural evolution of commercial aluminum alloy AA7050 in the solution treated condition (W) processed by ECAP. The analyses were made considering the effects of process parameters as temperature ( $T_{amb}$  and 150°C), processing route (A and B<sub>C</sub>) and number of passes. Optical microscopy (OM), scanning electron microscopy (SEM) and transmission electron microscopy (TEM) were used for microstructural characterization, and hardness tests for a preliminary assessment of mechanical properties. The results show that the refining of the microstructure by ECAP occurred by the formation of deformation bands, with the formation of dislocations cells and subgrains within these bands. The increase of the ECAP temperature led to the formation of more defined subgrains contours and intense precipitation of  $\eta$  phase in the form of spherical particles. The samples processed by Route B<sub>C</sub> present a more refined microstructure.

**Key words:** aluminum alloy; ECAP; microstructure

<sup>1</sup> First TMS-ABM International Materials Congress, Symposium: Mechanical Properties of Materials with Emphasis on Grain-Size Effects, July 26-30, 2010 – Rio de Janeiro, Brazil

<sup>2</sup> Materials Science and Engineering, Dr – UNIVAP

<sup>3</sup> Materials Engineering, undergraduate student - UNIVAP

<sup>4</sup> Biomedical Engineering, Dr – UNVAP

<sup>5</sup> Metallurgy and Science of Materials, Dr – UFSCar

<sup>6</sup> Materials Science and Engineering, Dr – UFSCar

## 1 INTRODUCTION

Severe plastic deformation (SPD) techniques have been widely used for the production of ultra fine grained microstructures in metal and alloys <sup>(1,2)</sup>. Among the various SPD processes available, equal channel angular pressing, ECAP is especially attractive because it is the most cost effective and easiest way due to the simplicity of process and tooling and because it can be scale-up to produce bulk ultra fine grained materials for structural applications. The process allows materials to undergo severe shearing deformation and break up the original texture into ultrafine or nanostructure after a number of passes of pressing through a die composed by two channels that intersect in an angle usually of 90° or 120° <sup>(1-4)</sup>. The process imposes a high strain on the sample so that a high dislocation density is introduced. These dislocations rearrange during the multiple passes of ECAP to form subgrains and subsequently new high angle grain boundaries.

Investigation of ECAP processing of precipitation-hardened Al alloys was primary focused on the process refinement <sup>(5-8)</sup> and more recently on the evolution and controlling of precipitation microstructure <sup>(9-13)</sup>. Previous studies <sup>(4, 14)</sup> have reported that different microstructures can be obtained in Al and Al alloys dependent upon the ECAP route. Gholinia et al <sup>(5)</sup> have demonstrated that during deformation with a constant strain path the grains in the alloy subdivide by the buildup of misorientations between cell blocks as the strain increases. This leads to the formation of elongated subgrains. When a billet is processed with a clockwise and anticlockwise 90° rotation, between each alternate pressing, this results in the continual buildup of shear on two mutually orthogonal planes. This is the less efficient route to produce submicron grains <sup>(5)</sup>. With a 90° rotation in the same direction, the billet is again sheared in two mutually orthogonal planes, but despite the redundant nature of the total strain, this processing route gives rise to grain refinement <sup>(5)</sup>.

ECAP process has a complicated effect on precipitation microstructure of Al alloys. It has been reported that ECAP at ambient temperature suppress the precipitation in alloy in the as quenched condition <sup>(10)</sup>, while ECAP at elevated temperature can cause dissolution of pre-existing metastable precipitates or precipitation in the case of the as quenched alloy <sup>(9)</sup>. A morphological change have been reported in Al-Zn-Mg-Cu alloys <sup>(15)</sup>, where spherical precipitates form by fragmentation of pre-existing large platelet precipitates, or by isotropic growth of small platelet precipitates <sup>(11)</sup>.

This work has the aim to investigate the microstructural evolution of AA7050 aluminum alloy in the solution treated condition (W) during ECAP. The effect of some processes variables will be considered, such as: temperature, processing route and number of passes, in the development of grain structure and precipitation state and thus provide additional information in the understanding of the behavior of this aluminum alloy during ECAP.

## 2 EXPERIMENTAL PROCEDURES

The AA7050 aluminum alloy, with nominal composition showed in Table 1, was received as plate in the condition T7451. Prior to ECAP, short billets were machined from the plate with lengths of 90 mm and diameter of 10 mm. The billets were solution treated at 477°C for 1 h and were processed by ECAP at ambient temperature and at 150°C with one, three and six passes.

The ECAP facility have an internal angle of 120° and an additional angle of 60° at the outer concordance radius where the two channels intersect. The ECAP processing was performed using a mechanical press of 30 tons with ram speed of 0.5 mm/s. The pressings were performed by routes A (sample is not rotated) and B<sub>C</sub> (sample is clockwise rotated by 90°).

Microstructural characterization of the samples after ECAP was performed by OM, SEM and TEM. Samples for OM and SEM were prepared by conventional techniques of metallographic preparation. For TEM characterization, thin foils of the material were cut from the cross-section of the each billet perpendicular to the pressing direction. The foils were thinned to 100 μm by conventional grinding. 3 mm discs were punched from the specimens and after that, they were ion-milled in a Gatan Dual Ion Milling System, using argon, bean energy of 5 keV.

Rockwell B hardness tests were performed in all samples for a preliminary assessment of mechanical properties.

**Table 1.** Nominal Composition of AA7050 aluminum alloy (AMS 4050 specification <sup>(16)</sup>).

Composition Weight %	AA7050									
	Zn	Cu	Mg	Zr	Fe	Si	Mn	Ti	Cr	Others (total)
Min.	5,7	2,0	1,9	0,08	-	-	-	-	-	-
Max.	6,7	2,6	2,6	0,15	0,15	0,12	0,10	0,06	0,04	0,15

### 3 RESULTS AND DISCUSSION

Only one pass of ECAP was possible at ambient temperature due to the sample low ductility. Figure 1(a) shows the OM microstructure of the alloy in the W condition. Figures 1(b) and 1(c) show microstructures obtained by OM and SEM, respectively, after one pass of ECAP at ambient temperature. Comparing these pictures, one can see that after 1 pass of ECAP the samples present a more refined and elongated grain structure. Deformation bands can be observed in the interior of some grains. As it has been previously reported <sup>(17,18)</sup>, deformation bands develop because it is energetically easier for a constrained grain to deform by splitting into bands (or cell blocks) that deform on fewer than the five slip systems required for homogeneous deformation. The formation of new high angle grain boundaries induced by deformation can occur if the misorientations between the deformation bands increase sufficiently.

Figure 2 shows TEM micrographs of alloy after one pass of ECAP at ambient temperature. It can be observed an elongated cell substructure with approximate width of 400 nm and a high density of dislocations arranged in the cell boundaries. No precipitation was observed after one pass of ECAP at ambient temperature.

Figure 3 shows micrographs of alloy processed at 150°C by route A. An intense refining of microstructure was observed after one pass of ECAP. After three and six passes a large amount of deformation bands was observed and they were homogeneously distributed throughout the sample. The number of these bands increased with the number of passes, while the average spacing between bands seems had decreased.

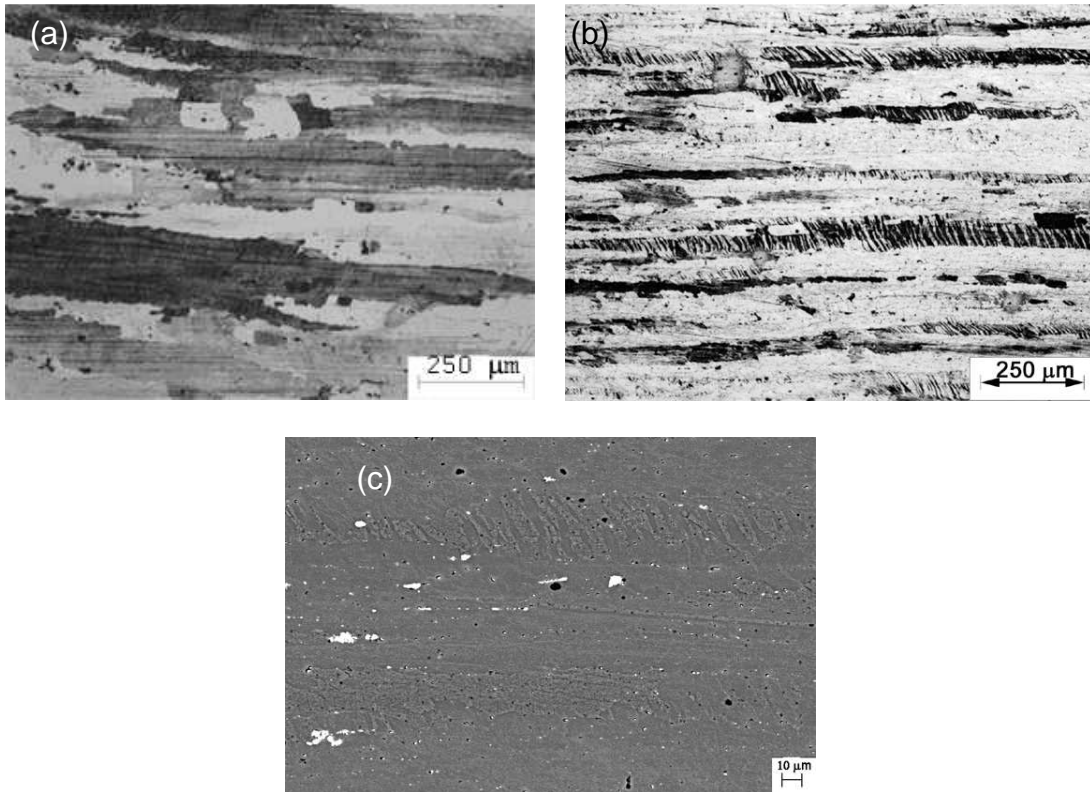


Figure 1. (a) Microstructure of 7050Al alloy in W condition. (b) and (c) Microstructures of 7050Al alloy after one pass of ECAP at  $T_{amb}$ , OM and SEM, respectively.

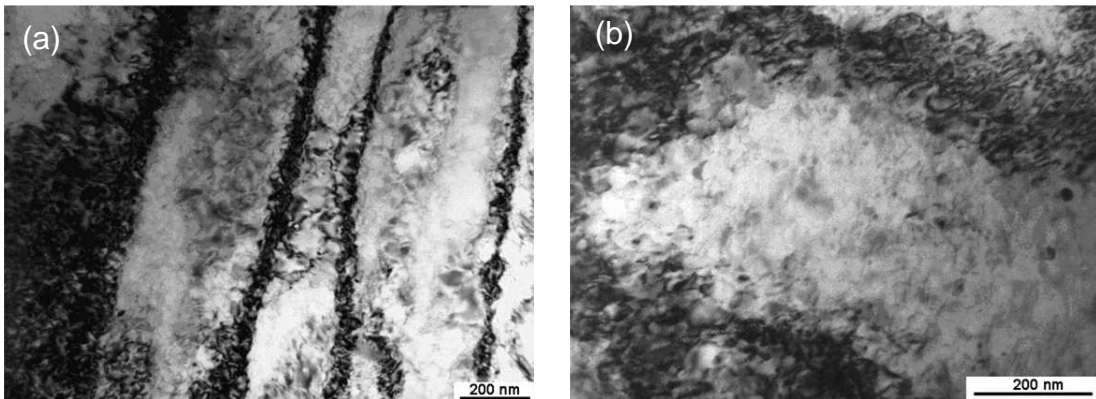


Figure 2. Bright field TEM images of 7050Al alloy after one pass of ECAP at  $T_{amb}$ .

Figure 4 shows OM and SEM micrographs of 7050Al alloy after ECAP by route B<sub>C</sub>. The microstructure is more refined as compared with samples with same number of passes pressed by route A. Deformation bands are visualized in minor number and the average spacing between bands seems to be smaller.

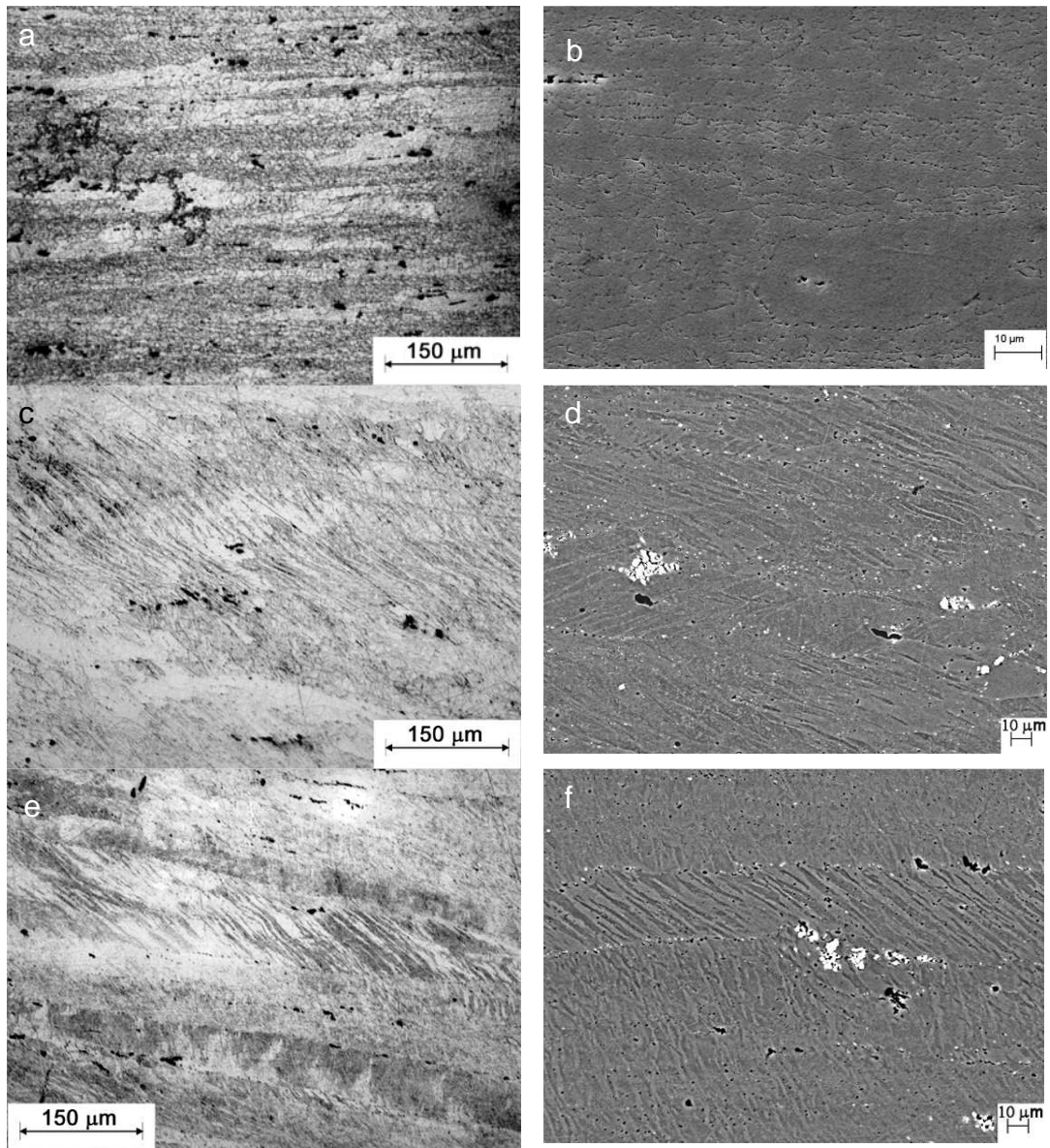


Figure 3. Microstructure of 7050Al alloy after ECAP at 150°C by route A. (a) and (b) one pass; (c) and (d) three passes; (e) and (f) six passes. (a), (c), (e) OM; (b), (d), (f) SEM.

Figure 5 presents the microstructure by TEM after ECAP at 150°C by Route A and B<sub>C</sub>. After one pass of ECAP at 150°C the microstructure is very similar of the sample pressed at ambient temperature, it is formed by elongated cells with average width of 200 nm and a high density of dislocations arranged in the cell boundaries.

The samples pressed by route A, for three and six passes, present the microstructure composed by elongated subgrains. After three passes the subgrains have an approximate width of 200 nm, while after 6 passes the subgrains are slightly smaller with a width of 100 to 200 nm. The subgrains contours of this sample are better defined than those obtained after one pass that presented thicker walls. The microstructure of samples after ECAP by route B<sub>C</sub> is formed by subgrains or cells with an equiaxial tendency and smaller than that of route A. High density of dislocations is present, located at cell boundaries.

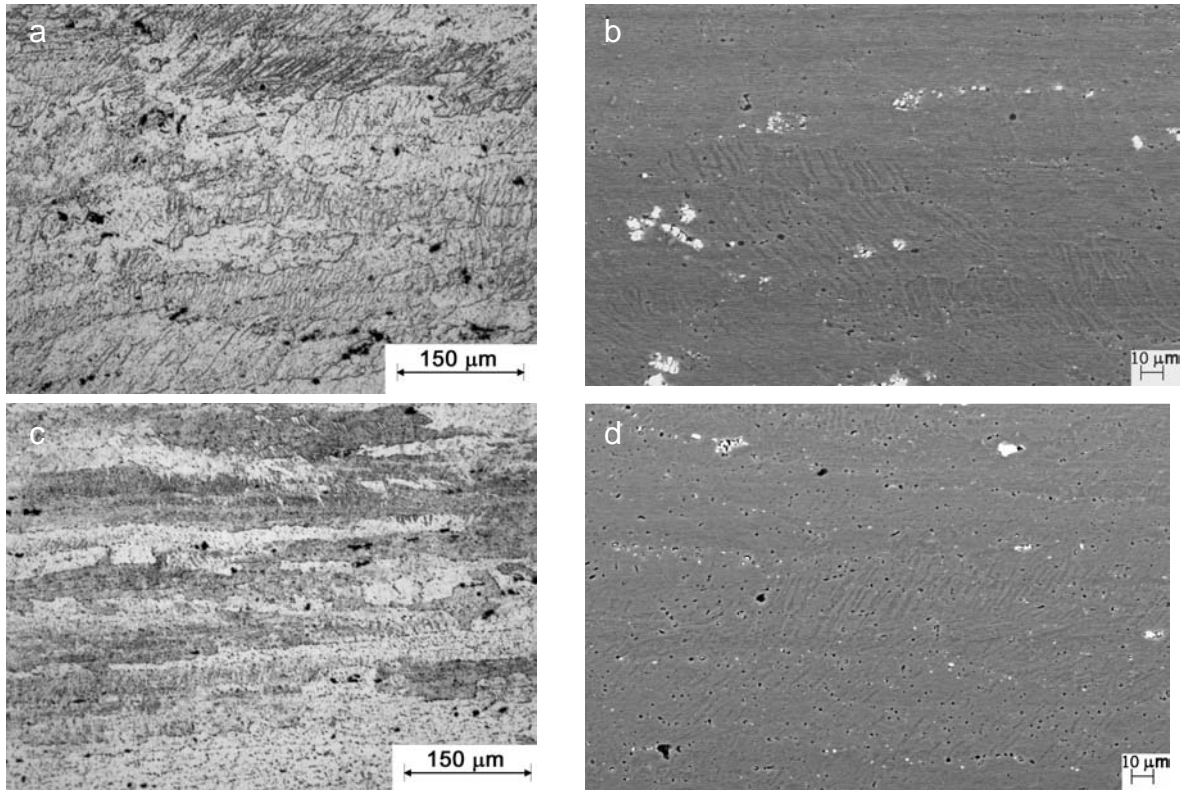


Figure 4. Microstructure of 7050Al alloy after ECAP at 150°C by route B<sub>c</sub>. (a) and (b) three passes; (c) and (d) six passes. (a), (c) OM; (b), (d) SEM.

A high density of precipitates was observed after processing at 150°C independently of the route. Figure 6 shows representative micrographs of precipitation state in the alloy pressed by ECAP. The sample after one pass presented high density of platelet precipitates with aspect ratios  $\leq 5:1$  (Figure 6a). The largest precipitates were  $\sim 100$  nm long and  $\sim 30$  nm thick, with aspect ratio close to 3:1. There was a significant change in the microstructure after three and six passes. The precipitates are now equiaxed and smaller than that of sample pressed for one pass. The diameters of precipitates are around 10 nm. EDS spectrum was obtained in STEM mode from particles (Figure 6d) and shows that the precipitates are composed by Mg, Cu and Zn.

The precipitation microstructures formed in ECAP of the 7050 Al alloy are very different from those formed after thermal ageing. After one pass, platelet precipitates, probably  $\eta$  phase, are observed. It has been reported<sup>(11)</sup> the presence of intermediate precipitates  $\eta'$  after the first pass of ECAP, which have taken to supposition that the precipitation during ECAP follows the same sequence as in a conventional ageing treatment (i.e. GP zones,  $\eta'$ ,  $\eta$ ), but that precipitation occurs in a faster rate. Although the usual platelet morphology of the  $\eta$  precipitates observed after the first pass of ECAP of 7050Al alloy, their aspect ratio are lower than that obtained by ageing. This lower aspect ratio can be explained by the orientation changes that ECAP produces on precipitates, which increases the interfacial energy between precipitates and matrix<sup>(11)</sup>. The small precipitates are more sensitive to the change in interfacial energy, so, adopting low aspect ratios, these small platelet precipitates reduce their surface area.

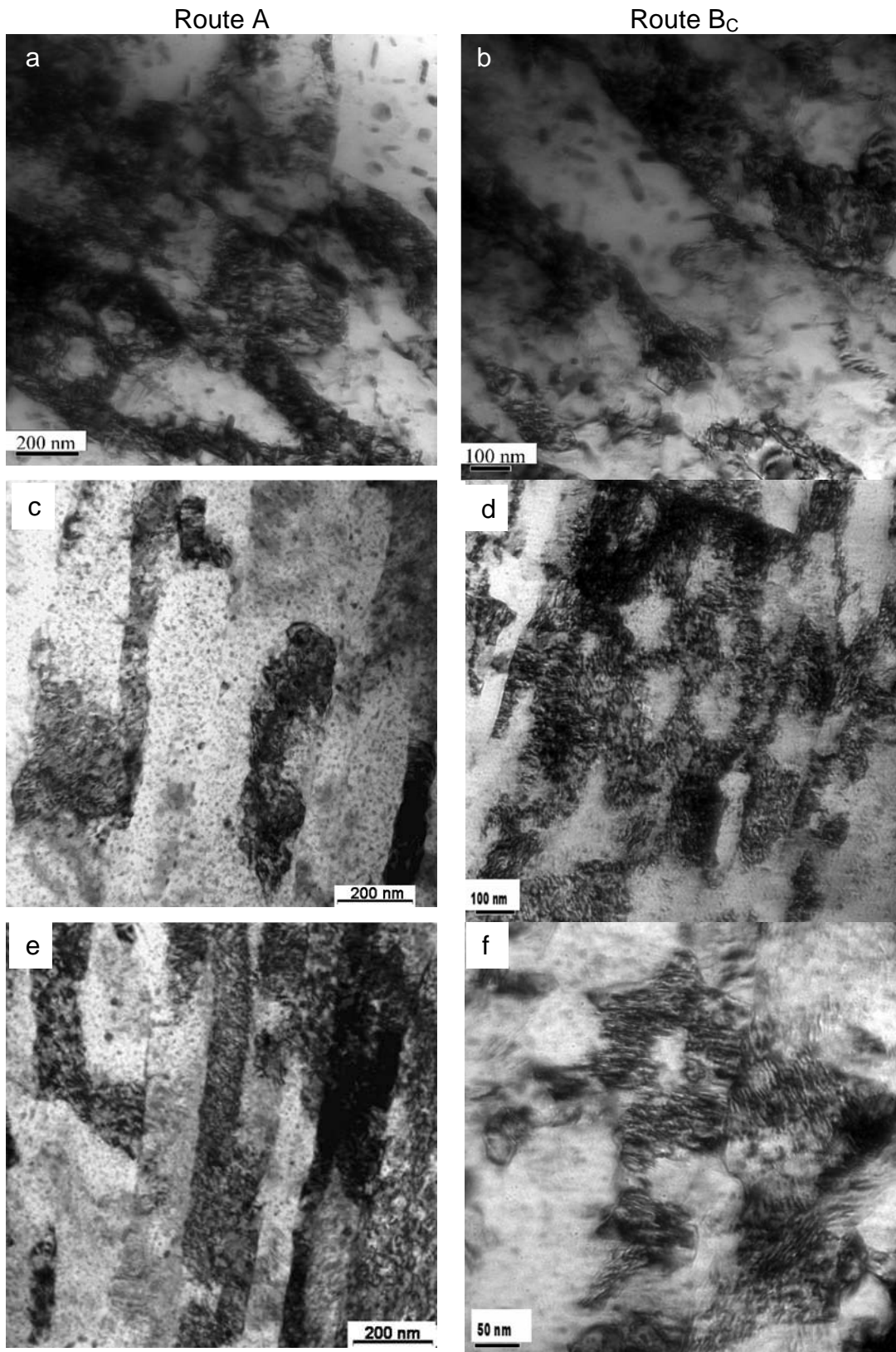


Figure 5. Microstructure by TEM of 7050Al alloy after ECAP at 150°C. (a) and (b) one pass; (c) and (d) three passes; (e) and (f) six passes.

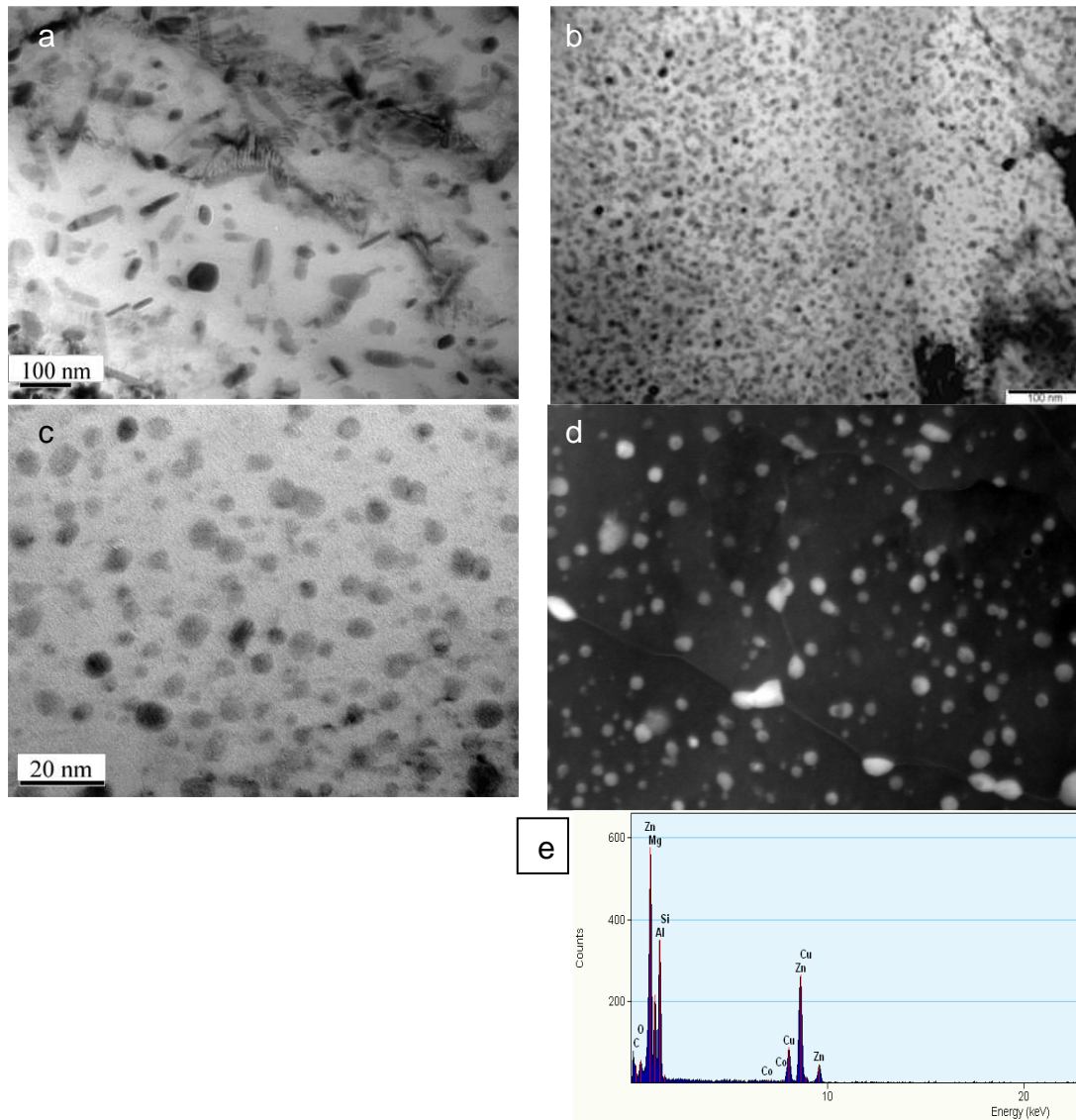


Figure 6. Microstructure by TEM of 7050Al alloy after ECAP at 150°C. (a) one pass; (b) three passes by route A (TEM); (c) six passes by route B<sub>C</sub> (BF – STEM); (d) six passes by route B<sub>C</sub> (HAADF image); (e) EDS spectrum of particle indicated in (d).

After multiple passes the precipitates present in the 7050Al alloy are the equiaxed  $\eta$  precipitates. This change in morphology can have been caused by isotropic growth promoted by the rotations after multiple passes. Since the new orientations of precipitates within the matrix deviate from the typical orientation for  $\eta$  platelet, the atomic configurations at the interphase interfaces are different. The missing low energy configuration interface between the basal plane of  $\eta$  phase and  $\{111\}$  of the Al matrix increases the interfacial energy between  $\eta$  and Al. Thus the  $\eta$  precipitates become more favorable for isotropic growth and they evolve into equiaxed morphology<sup>(11)</sup>. However, as the precipitates particles after three and six passes of ECAP are smaller than that after the first pass, besides the isotropic growth of precipitates, the fragmentation of the larger particles should play a major role in the precipitation evolution, and this process should be responsible for the spheroidization of precipitates during ECAP.

Table 2 shows the hardness values in Rockwell B scale for all conditions of ECAP used in this work. ECAP caused an accentuated increase of alloy hardness compared with the initial condition W ( 37 HRB). The increase of hardness should be resulted from precipitation and work hardening during ECAP. It was observed a slight decrease of hardness with increase of number of passes of ECAP. This behavior must be resulting from recovering process during ECAP at 150°C. No relevant differences were observed between samples pressed by routes A or B<sub>C</sub>.

**Table 2.** Rockwell B Hardness of 7050Al alloy after ECAP

Initial Sample Condition	Solution Treated (W)						
	-	Route A			Route B <sub>C</sub>		
Route	-	150°C			150°C		
Temperature	T <sub>amb</sub>	150°C			150°C		
Number of passes	1	1	3	6	1	3	6
HRB	87	88	93	88	88	93	92

#### 4 CONCLUSIONS

In this work the commercial AA7050 aluminum alloy in the solution treated condition (W) was processed by ECAP to examine the effects of process parameters as temperature (T<sub>amb</sub> and 150°C), processing route (A and B<sub>C</sub>) and number of passes, in the development of the microstructure of the alloy during pressing.

Processing by ECAP leads to a refined microstructure by the formation of deformation bands, with the formation of dislocations cells and subgrains within these bands, with sizes of about 200 nm. The increase in the number of passes of ECAP leads to further refining of microstructure. The samples processed by Route B<sub>C</sub> present a more refined microstructure.

The increase of the ECAP temperature led to intense precipitation of η phase in the form of platelet particles after one pass of ECAP that evolve to spherical morphology after multiple passes.

ECAP caused an accentuated increase of alloy hardness resulted from precipitation and work hardening. A slight decrease of hardness with increase of number of passes of ECAP must be resulting from recuperation process during ECAP at 150°C. No relevant differences were observed between samples pressed by routes A or B<sub>C</sub>.

#### ACKNOWLEDGEMENTS

The authors would like to acknowledge the financial support of FAPESP, process number 2005/03440-5.

#### REFERENCES

- 1 SEGAL, V.M. Mater. Sci. Eng. A 197, p .157, 1995.
- 2 VALIEV, R.Z., ISLAMGALIEV, R.K.; ALEXANDROV, I. V. Progress in Materials Science, v. 45, p. 103, 2000.
- 3 VALIEV, R.Z., KORZNIKOV, A.V., MULYUKOV, R.R., Mater. Sci. Eng. A 168, p .141, 1993.

- 4 IWAHASHI, Y., WANG, J., HORITA, Z., NEMOTO, M., LANGDON, T.G., Scripta Mater. 35, p .143, 1996.
- 5 GHOLINIA, A., PRANGNELL, P.B., MARKUSHEV, M.V., Acta Mater. 48, p.1115, 2000.
- 6 FURUKAWA, M., HORITA, Z., LANGDON, T.G., Journal of Materials Science 40, p.909, 2005.
- 7 IWAHASHI, Y., HORITA, Z., NEMOTO, M., LANGDON, T.G., Acta Mater. 45, p .4733, 1997.
- 8 STOLYAROV, V.V., LATYSH, V.V., SHUNDALOV, V.A., SALIMONENKO, D.A., ISLAMGALIEV, R.K., VALIEV, R.Z., Mater. Sci. Eng. A 234-236, p.339, 1997.
- 9 MURAYAMA, M., HORITA, Z., HONO, K., Acta Mater. 49, p.21, 2001.
- 10 ZHAO, Y.H., LIAO, X.Z., JIN, Z., VALIEV, R.Z., ZHU, Y.T., Acta Mater. 52, p.4599, 2004.
- 11 SHA, G., WANG, Y.B., LIAO, X.Z., DUAN, Z.C., RINGER, S.P., LANGDON, T.G., Acta Materialia 57, p. 3123, 2009.
- 12 GUBICZA, J., SCHILER, I., CHINH, N.Q., ILLY, J., HORITA, Z., LANGDON, T.G., Mater. Sci. Eng. A 460-461, p.77, 2007.
- 13 RADETIC, T., POPOVIC, M., ROMHANJI, E., VELINDEN, B., Mater. Sci. Eng. A 527, p.634, 2010.
- 14 IWAHASHI, Y., HORITA, Z., NEMOTO, M., LANGDON, T.G., Acta Metall. 46, p. 3317, 1998.
- 15 XU, C., FURUKAWA, M., HORITA, Z., LANGDON, T.G., Acta Mater. 53, p.749, 2005.
- 16 Aerospace Material Specification 4050, SAE International,
- 17 APPS, P. J., BOWEN, J. R., PRANGNELL, P. B., Acta Mater 51, p. 2811, 2003.
- 18 PRANGNELL, P.B., BOWEN, J.R., APPS, P.J., Mater. Sci. Eng. A 375-377, p. 178, 2004.